TIME VARIABILITY OF THE He I 10830 Å LINE PROFILE

JAGDEV SINGH, S. K. JAIN, and P. VENKATAKRISHNAN
Indian Institute of Astrophysics, Bangalore 560034, India

(Received 5 November, 1992; in revised form 8 November, 1993)

Abstract. We have studied the time-dependent behaviour of the He I 10830 Å line. These studies show that (i) the fluctuations of the line width are uncorrelated with the equivalent-width fluctuations and (ii) the autocorrelation curves for the equivalent-width fluctuations are broader than those for line-width fluctuations. These results could be interpreted as the signatures of the eruption of density inhomogeneities, like spicules, into the altitudes of formation of the He I 10830 Å line.

1. Introduction

The excitation of the He I 10830 Å line by back radiation from coronal UV radiation provides a ground-based technique for mapping coronal structures. In an earlier paper (Venkatakrishnan *et al.*, 1992, hereinafter referred to as Paper I), the time-averaged spatial variation of the equivalent width of the He I 10830 Å line was shown to be produced mainly by spatial variation in the coronal radiation. In the same paper, the variance of the temporal fluctuation of the line parameters was also studied as a function of the mean equivalent width. It was seen that the r.m.s. fluctuation of the equivalent width and line depth increased with the mean value of the equivalent width. On the other hand, the r.m.s. fluctuation of the Doppler shift and line width were smaller at regions of large mean equivalent width compared to the r.m.s. value at weak line regions.

The cause of the time-dependent fluctuations could not be precisely identified. Fluctuations in the UV radiation flux were suggested to be one reason, while eruption of spicules into the region of line formation was another possibility. In this paper, we attempt a firmer identification for the cause of the observed equivalent width fluctuations, based on a more detailed examination of the time dependence of the line parameters. In Section 2 we present the results while in Section 3 we discuss the implications of these results.

2. Results

Basically, the data consists of a time series of spectra, taken in the region of the He I 10830 Å line using the 512 channel magnetograph (Livingston *et al.*, 1976) of the National Solar Observatory at Kitt Peak, Arizona. The details of the observation and data reduction have been reported in Paper I. In the present paper we focus our attention on the first one-hour stretch of the time series obtained on 20 January, 1985, and 72 min series on 2 June, 1986. The binning of two pixels into one data point and the correction for solar rotation allows us to consider 250 contiguous

Solar Physics **150:** 49–59, 1994.

spatial locations on the solar disc, each having an effective pixel size of 1 arc sec by 2 arc sec. The spectra were sampled at the rate of one per minute providing us with 60 spectra for each spatial location on 20 January, 1985, and at the rate of one every 30 s on 2 June, 1986 for 72 min, yielding 144 spectra for each spatial location for the present study.

In Paper I we had presented results on four line parameters, viz., the equivalent width, the line depth, the Doppler shift (wavelength shift of the centre of gravity of the line from a reference wavelength) and the line width (full width at half maximum of the line profile).

Most of Paper I dealt with time averages of the line profile parameters. In this paper we wish to address the time variation of the parameters. For this we will have to look at individual profiles, where the signal-to-noise ratio becomes poorer. To arrive at an estimate for the noise in an individual spectrum, we monitored the fluctuations over a region of 2.86 Å from 10827.76 Å to 10830.62 Å. We first took a running average of the counts in this wavelength region and subtracted this from the original data. The trends were removed, leaving behind the higher-frequency fluctuations. The root-mean-square residual fluctuations gave a reasonably accurate estimate of the noise. This value turned out to be $\approx$0.25 counts over a mean continuum value of $\approx$140 counts. Applying a 3σ criterion for the line depth, we then rejected all data where the line depth is smaller than 0.006.

The error $\delta\eta$ in the line depth η will then be $\delta I/I_c$ which, in our data reduces to $\lesssim$0.002. The error δq in the equivalent width, q, will be less than $\delta\eta$, since q is determined from the relative intensities at several positions in the line profile.

The error $\delta\lambda$ in the line width, $\Delta\lambda$, which is determined using the intensity criterion of full width at half maximum, is given by $\sqrt{2\delta I(\partial I/\partial\lambda)^{-1}}$, where δI is the error fluctuation in the intensity and $\partial I/\partial\lambda$ is the slope of the profile at half maximum. Now, $\partial I/\partial\lambda \approx \eta I_c/2\Delta\lambda$, where η is the line depth and I_c is the continuum value. Thus, the error in the determination of the line width turns out to be $\delta\lambda \approx 2(\sqrt{2\Delta\lambda}/\eta)\,(\delta I/I_c)$ which for our data reduces to

$$\delta\lambda \approx 0.005\Delta\lambda/\eta\,. \tag{1}$$

Since the values of η range from 0.012 to 0.11, we find that the error in $\Delta\lambda$ ranges from $\approx$42% for the weak profiles to $\approx$4% for the strong profiles. With this background on the errors, let us now look at the temporal behaviour of the data.

Figures 1(a–c) show the line depth and line width plotted as a function of equivalent width in panel A and B, respectively, at three different locations on the Sun. The individual points represent the values obtained from spectra taken at different times over a single spatial pixel of $1'' \times 2''$. Figure 1(a) represents a typical example of a weak profile, where the equivalent width variations with time range between 0.01–0.03 Å. The mean equivalent width at that location is seen to be $\approx$0.02 Å, which represents a good signal to noise ratio. Figure 1(b) shows an example of a profile of intermediate strength in which the equivalent width variation

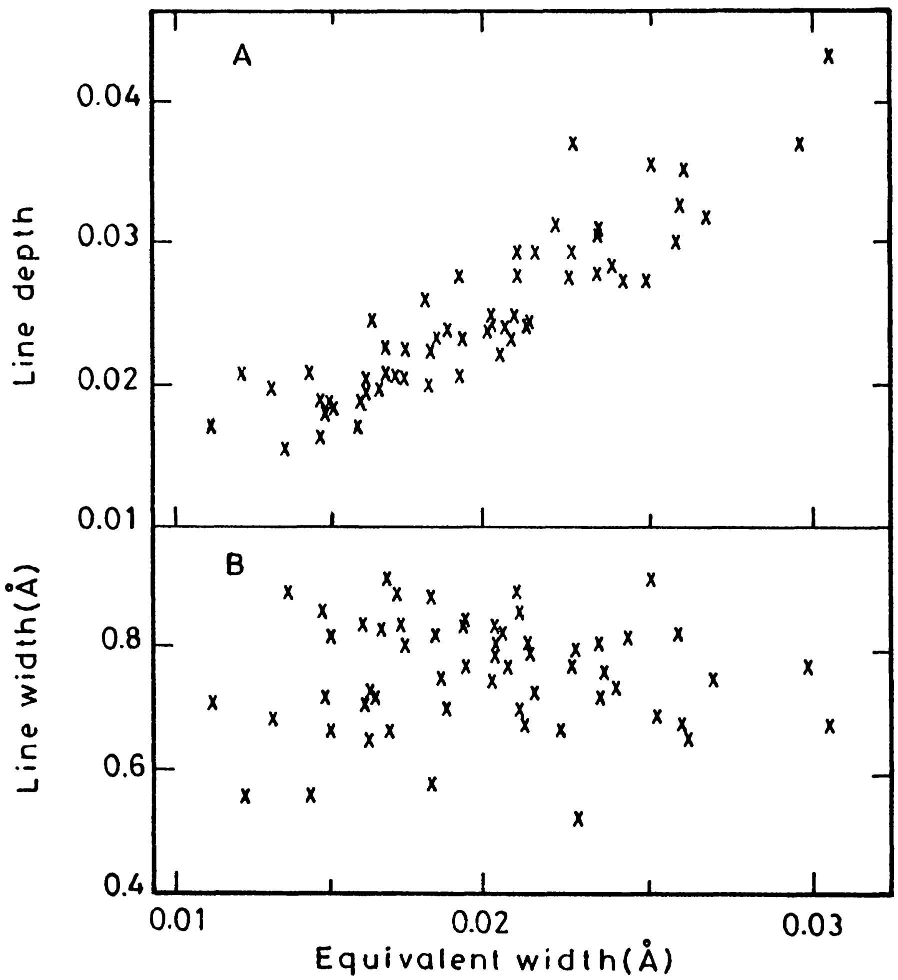

Fig. 1a. The variation of line depth (A) and line width (B) with equivalent width is shown. Each point, represented by a '×', denotes the line parameters derived from one spectrum of the time series obtained on January 20, 1985 for pixel number 25 having a time-averaged equivalent width of 0.02 Å.

with time ranges between 0.02–0.05 Å. The variations in equivalent width with time for a strong profile are shown in Figure 1(c).

These figures indicate that the range in variation of the line depth is ≈0.03 for weak profiles, 0.04 for profiles of intermediate strengths and 0.06 for strong profiles. This range of variation in line depth is far greater than the expected noise fluctuation (<0.002). The line depth fluctuation is also seen to follow the equivalent width fluctuation very faithfully.

Figures 1(a–c) show that the mean line width increases marginally with the increase in equivalent width. The mean equivalent width at different locations on the Sun differs by a factor of ≈4 whereas the change in mean line width is only ≈18%. These figures also indicate that mean line width averaged over time is ≈0.75 Å for weak profiles and ≈0.90 Å for strong profiles and variation in line width with time is ≈ ±0.15 Å. Taking 0.90 Å as the line width and 0.08 as the line depth (Figure 1(c)) at that location, Equation (1) tells us that the expected noise fluctuation in the line width is ≈0.05 Å. The observed variation of ≈ ±0.15 Å

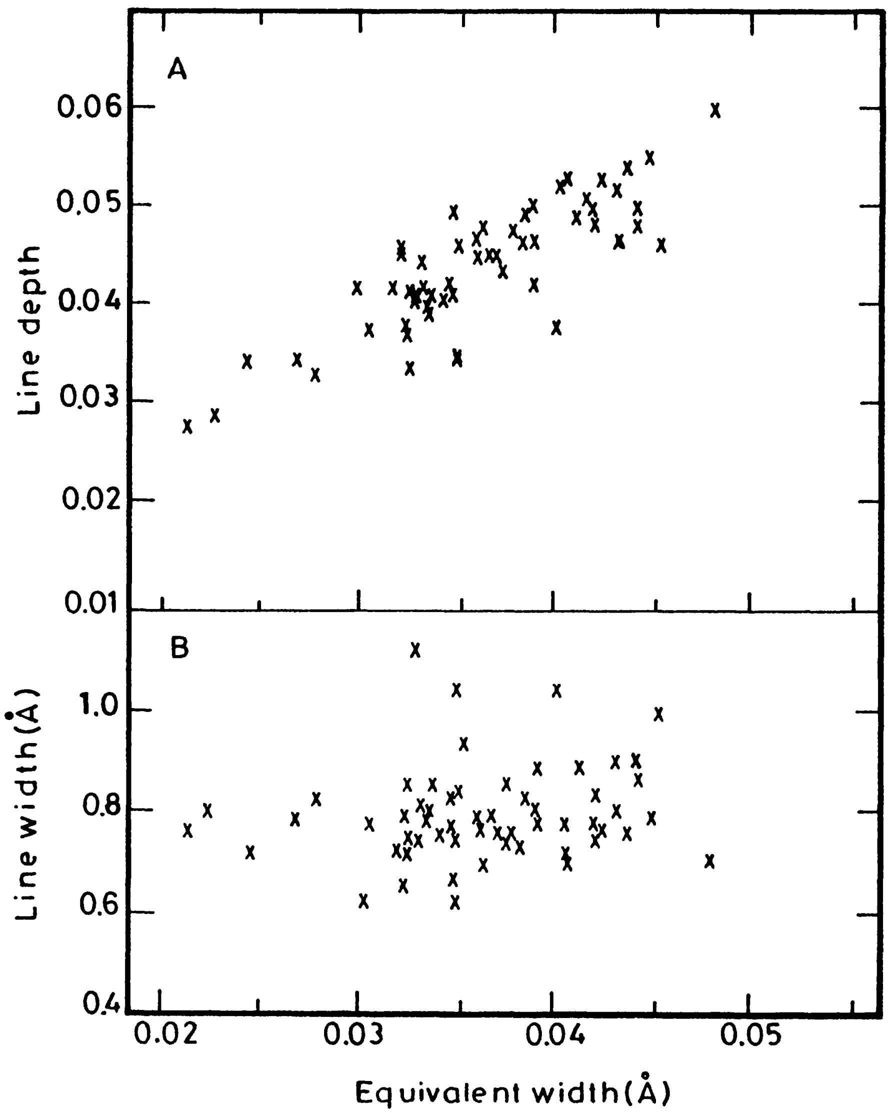

Fig. 1b. Same as Figure 1(a) but for pixel number 98, with an averaged equivalent width of 0.035 Å.

is marginally significant at the 3σ level. Thus a single pixel observation tells us that the equivalent width and line depth variations are far above the errors of measurement while the line width variation is marginally above the noise.

The picture changes somewhat when we look at Figures 2(a–c) which are similar to Figure 1, but concern the spatially-averaged data for groups of 5, 5, and 7 contiguous pixels respectively in the vicinity of the single pixels of Figures 1(a–c). The overall time-averaged equivalent widths are 0.016, 0.028, and 0.072 Å for these locations with spatial resolution of $1'' \times 10''$, $1'' \times 10''$, and $1'' \times 14''$, respectively, for data shown in Figures 2(a–c). In this case, as seen from panels A of these figures, the line-depth variations once again follow the equivalent-width variations. However, the line width continues to vary at random around the mean values (panels B). The expected noise fluctuation in the line width is quite small, though, and is $\approx$0.02 Å for the strong profile and $\approx$0.05 Å for the profile

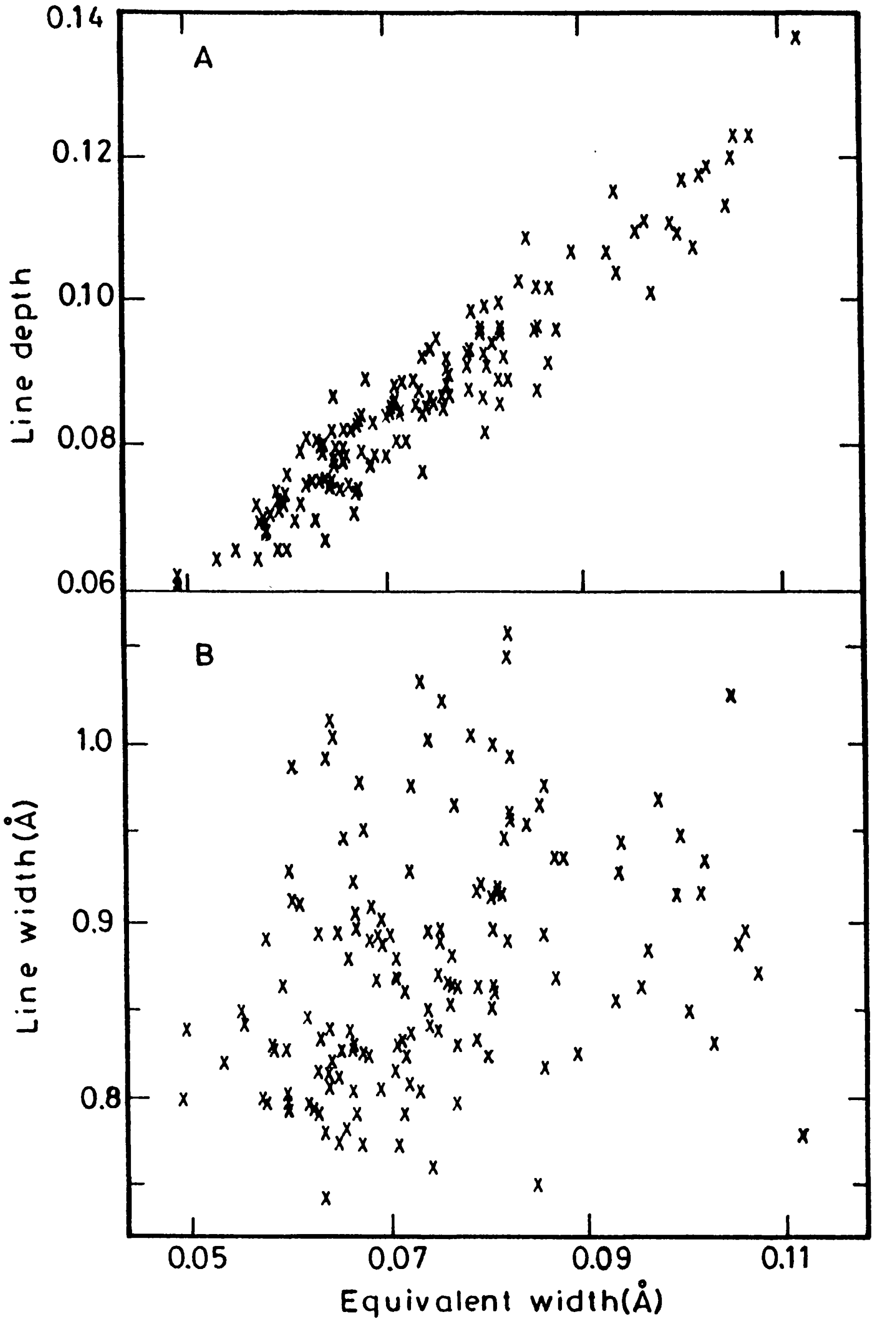

Fig. 1c. Same as Figure 1(a) but for spectra obtained on June 2, 1986; pixel number 128 with an averaged equivalent width of 0.08 Å.

of intermediate strength. This is because the combination of information from N pixels will decrease the noise to $\sqrt{N}$ times that for a single pixel. Even so, we see from panels B of Figures 2(a–c), that the amplitude of variations in line width continues to be of the same order as that for a single pixel. This indicates that the variations could have a solar origin. The point is that the slope in the scatter plot of line width versus equivalent width appears to be close to zero, while it is almost unity in the scatter plot of line depth versus equivalent width.

The above results are concerned with the cross correlation of the line parameters.

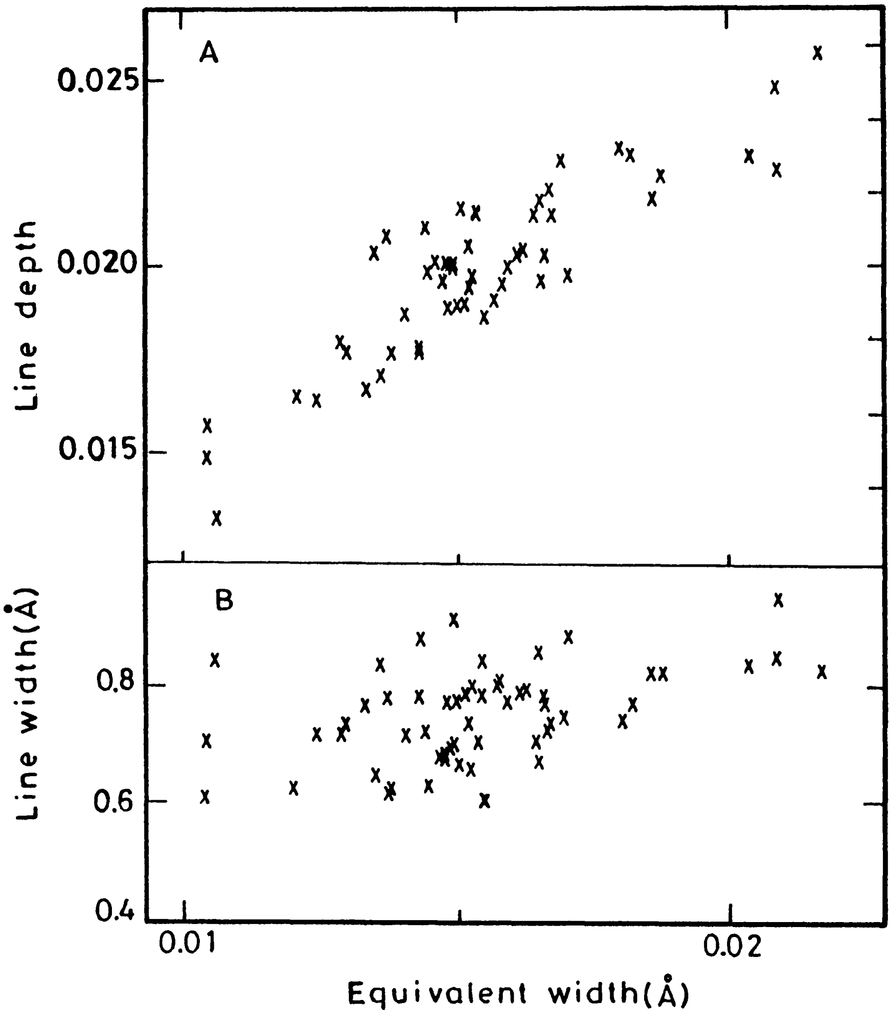

Fig. 2a. The variation of line depth (A) and line width (B) with equivalent width for time series spectra taken on January 20, 1985. Each data point represents the spatially-averaged parameters for a set of 5 contiguous pixels with an overall time-averaged mean equivalent width of 0.016 Å.

Let us now look at their individual time behaviour. Since the line depth and equivalent width are well correlated in time, we will examine the behaviour of the equivalent width alone and contrast it with the behaviour of the line width. In order to be able to compare the behaviour at different spatial locations, independent of phase factors, we calculated the autocorrelation function (AC function) at each location. At the pixel level, the AC function is very 'noisy' consisting of numerous peaks. We therefore summed up all the AC functions to produce a mean AC function where only the statistically significant and common features for all pixels will survive. Figure 3 shows such a mean AC curve for the equivalent-width (solid line) as well as the line-width (dashed line) variations. We see that the line-width AC curve drops down at a time lag of $\approx$1 min (which is the sampling interval). Thus the line-width fluctuations have no temporal coherence on scales larger than the sampling interval. The equivalent-width fluctuations, on the other hand, show enhanced power at lag intervals of 1 to 6 min.

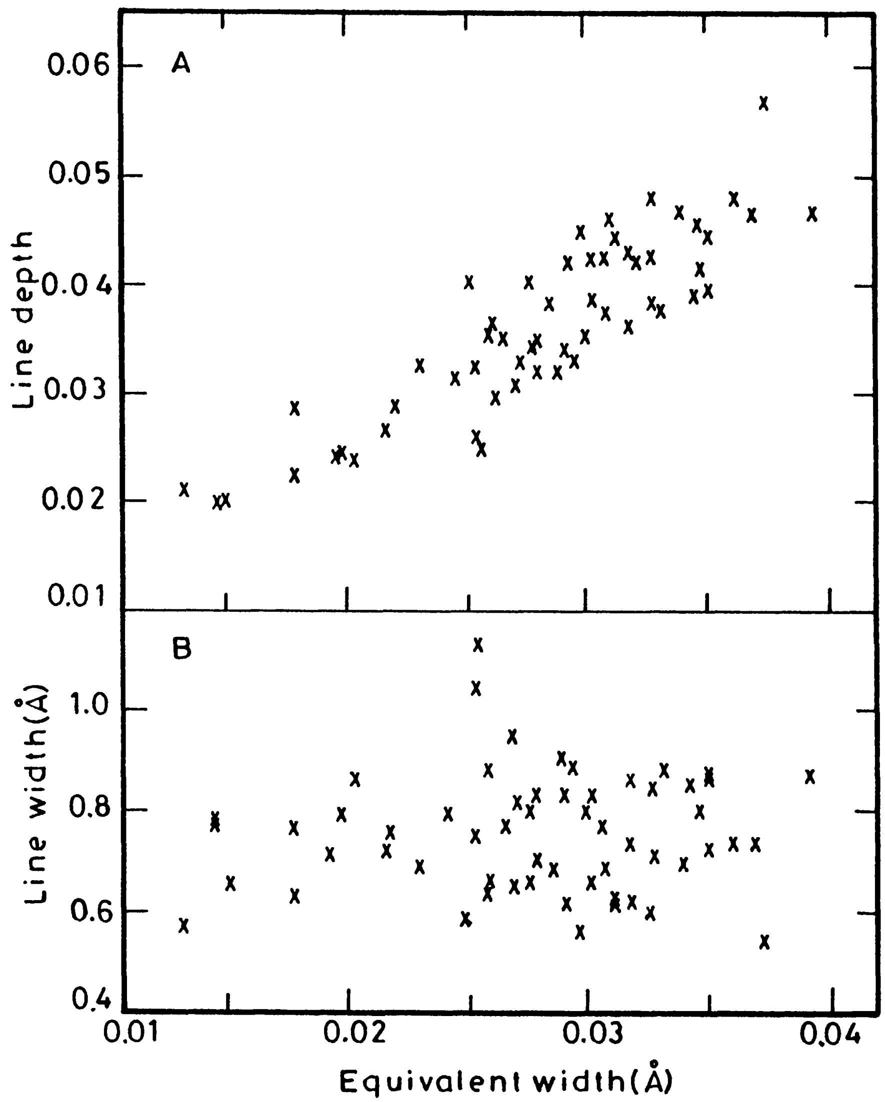

Fig. 2b. Same as Figure 2(a) but for another location with mean equivalent width of 0.028 Å.

3. Discussion

The chief result of this paper is that the time-dependent fluctuations of the line width are not correlated with the fluctuations in the equivalent width at any given spatial location. This result should be compared with that in Paper I where we found that the spatial variation of the line width was significantly related to the spatial variation of the equivalent width. Before we discuss the implications of the results of this paper, let us briefly review our understanding of the spatial variation of the line parameters as seen in Paper I.

The time-averaged equivalent width was seen in Paper I to vary by a factor of eight across different spatial locations. Such a variation can be induced either by a corresponding increase in the plasma density at these locations or by an increase in the excitation rate. An increase in the plasma density of more than 50% is ruled out from the empirical models of quiet network features (Vernazza, Avrett, and

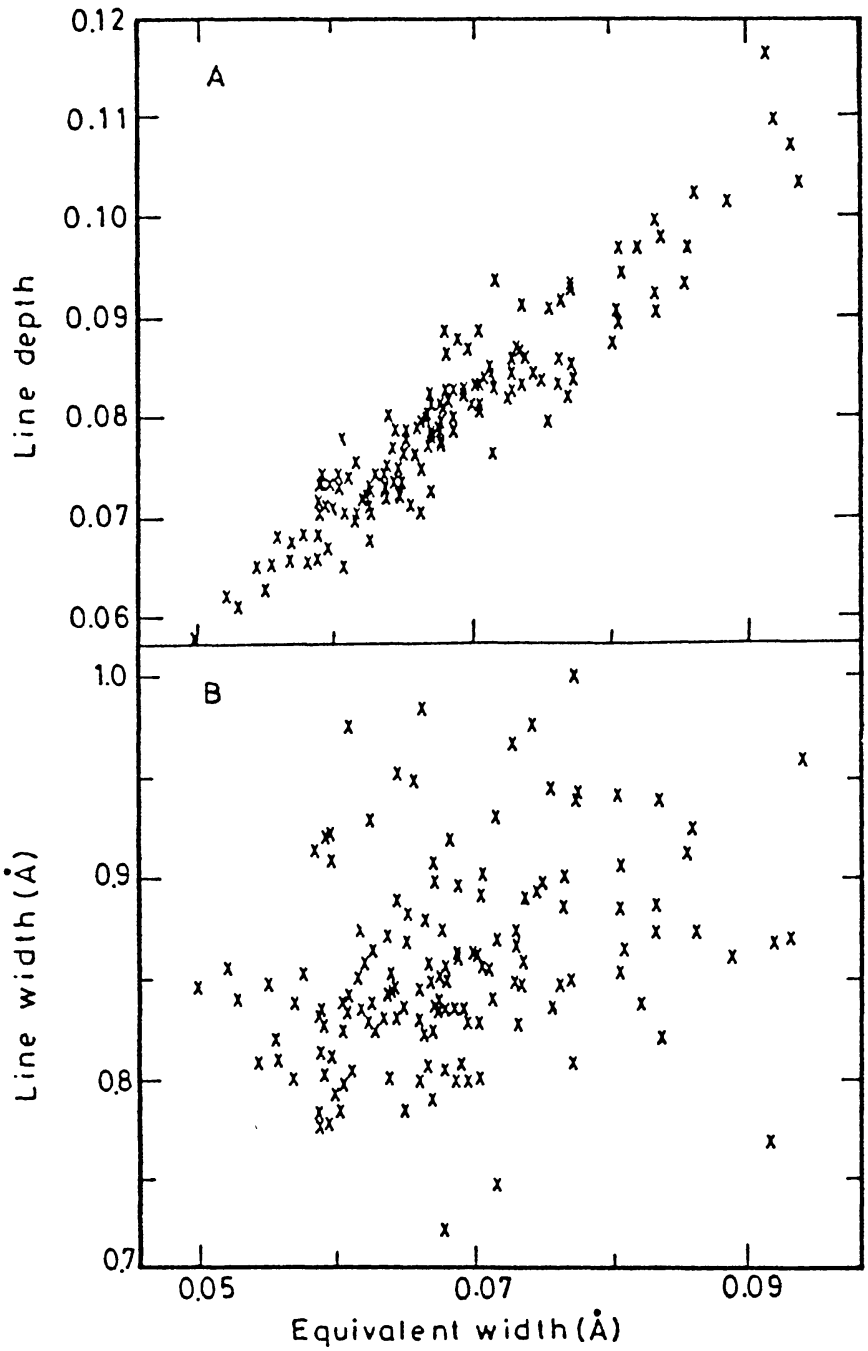

Fig. 2c. Same as Figure 2(a) but for spectra obtained on June 2, 1986. Here each data point represents mean of 7 contiguous pixels with an overall time-averaged equivalent width of 0.072 Å.

Loeser, 1981). Thus what remains is the possibility of an increase in the excitation rate. Collisional excitation is not possible since the thermal energy associated with the observed line width is far below the 20 eV required for exciting the He atom to the ^3S initial state of the 10830 Å line transition. Hence one must look for sources of radiative excitation, via the photoionization-recombination (PR) process (Zirin, 1989). The level of He I absorption is therefore an index of coronal EUV radiation. The increase in the time-averaged line width seen in Paper I accompanied by an

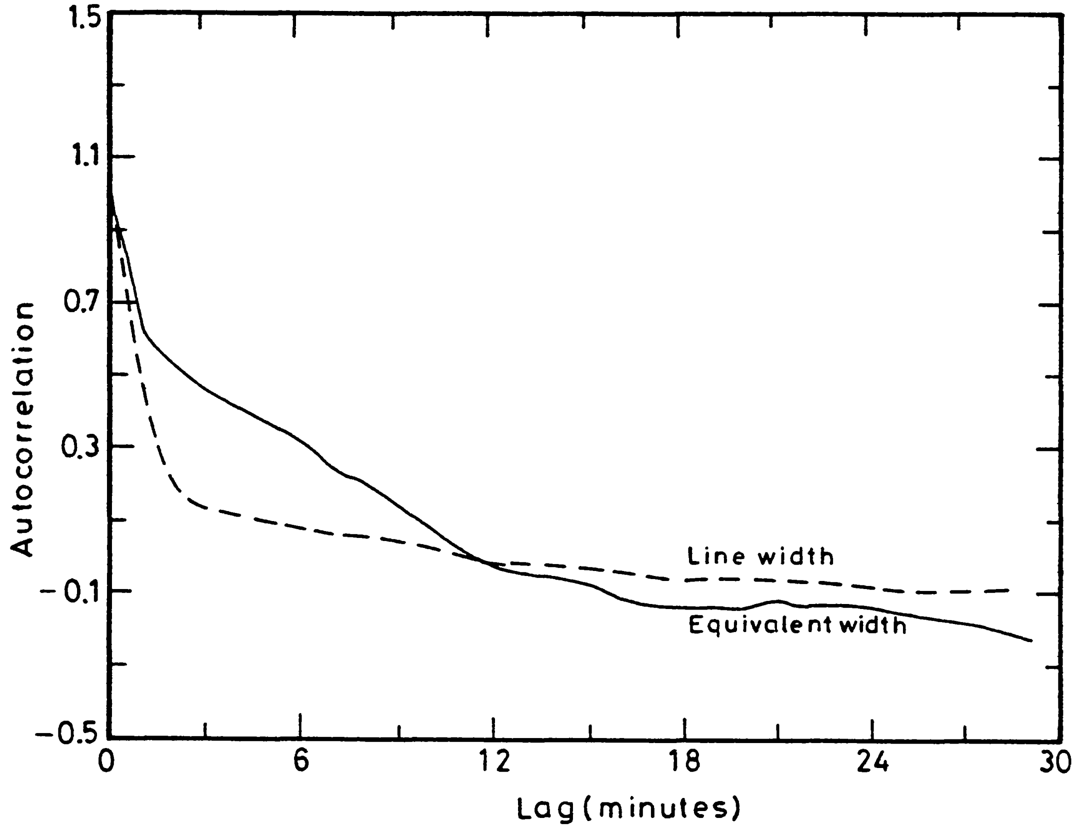

Fig. 3. The mean autocorrelation function of equivalent-width variations (solid line) and line-width variations (dashes) for all pixels plotted as a function of the time lag in minutes.

increase in the equivalent width indicates that chromospheric energy density is associated with coronal heating. It can be easily verified that the typical coronal radiative flux is far too low to increase the chromospheric plasma energy density to the level indicated by the observed line width. Thus, a proper interpretation of the correlation is that the enhanced chromospheric mechanical energy density causes an enhanced coronal EUV radiation (Venkatakrishnan, 1993). With this background on the spatial variation of the line parameters, let us now address the problem of their time variability at a given spatial location.

The fact that the line-width and equivalent-width fluctuations are not correlated in time clearly indicates that these fluctuations have independent origins. The spatial correlation seen in Paper I, however, constrains the possible explanations for the time variability of the equivalent width to some extent. For example, the time variability of the equivalent width could be attributed to a corresponding time variability in coronal radiation. The spatial correlation of the time-averaged chromospheric energy density with the coronal radiation, on the other hand, does require that the time variability of the line width should also be compatible with such a variable coronal heating. The lack of temporal correlation between line width and equivalent width rules out this possibility. To pursue a coronal origin for the equivalent width variation one would have to invoke separate mechanisms for the time-averaged heating of the corona in contrast to a time-dependent heating that does not involve variations in the chromospheric energy density.

Alternatively one can assume that the coronal heating is steady with small random fluctuations following the observed line-width fluctuations. The equivalent-width fluctuations must then be only due to density fluctuations. Since the amplitude of the equivalent-width fluctuation is $\leq 50\%$, the corresponding density fluctuations will be within the range prescribed by the empirical models of Vernazza, Avrett, and Loeser (1981).

How can such a density enhancement in the line of sight take place? A lateral compression of plasma columns would require a corresponding decrease in the density at adjacent pixels. This is not seen in the data. The only remaining possibility is for material to enter the line-forming heights from below. Spicules seem to be the natural candidates for doing this.

Spicules however reach velocities $\approx$20 km s^{-1} as seen in limb observations. The disc counterparts of spicules remain quite a mystery. In any case, the velocity data (Paper I; Lites, 1985) rule out any such velocity excursions. A simple reconciliation would be to assume that the acceleration to higher velocities occurs above the height of formation of the He I 10830 Å line. This then puts constraints on the physical domain of the line formation heights for reasons of consistency with the limb D_3 data. Furthermore, any time-dependent heating and cooling associated with the episodic ejection of spicular material must produce their signatures on the line width data on time scales consistent with the equivalent width fluctuations. Thus, whatever is causing the density inhomogeneities to erupt into the heights of formation of the He I 10830 Å line is not a predominantly time-dependent heating process. This leaves us with the problem of the origin of the line-width fluctuations. One can propose several explanations for these fluctuations. The existence of a multitude of temporal and spatial scales in a turbulent plasma provides a natural explanation. Departures of the line shapes from a gaussian distribution arising out of line asymmetrics or other similar reasons could also lead to line-width fluctuations.

In summary, we have shown that the time variation of the He I 10830 Å line parameters is consistent with eruption of density inhomogeneities into the region of line formation. These inhomogeneities are not accompanied by similar variations in the line width. Thus these inhomogeneities seem to be ejected by processes that do not involve a net heating or cooling of the material.

Acknowledgements

The visit of J. Singh to KPNO was financed by the Director, National Observatory, National Optical Astronomical Observatories, operated by the Association of Universities for Research in Astronomy, Inc., under contract with the National Science Foundation. A travel grant to J. Singh was provided by NSF. The criticisms of the referees have significantly contributed towards improving the paper.

References

Livingston, W. C., Harvey, J. W., Slaughter, C. D., and Trumbo, D.: 1976, *Applied Optics* **15**, 40.
Lites, B. W.: 1985, in H. U. Schmidt (ed.), *Theor. Prob. High Resol. Solar Phys.*, MPA 212, Münich, p. 273.
Venkatakrishnan, P.: 1993, *Solar Phys.*, in press.
Venkatakrishnan, P., Jain, S. K., Singh, J., Recely, F., and Livingston, W. C.: 1992, *Solar Phys.* **138**, 107 (Paper I).
Vernazza, J. E., Avrett, E. H., and Loeser, R.: 1981, *Astrophys. J. Suppl.* **45**, 635.
Zirin, H.: 1989, *Astrophysics of the Sun*, Cambridge University Press, Cambridge, p. 200.